Microsystem Technologies (2021) 27:2553–2566
https://doi.org/10.1007/s00542-020-05085-0

TECHNICAL PAPER

# Accurate position control of shape memory alloy actuation using displacement feedback and self-sensing system

Ermira Junita Abdullah[1] · Josu Soriano[2] · Iñaki Fernández de Bastida Garrido[2] · Dayang Laila Abdul Majid[1]

Received: 30 July 2020 / Accepted: 23 October 2020 / Published online: 7 November 2020


## Abstract

Numerous shape memory alloy (SMA) linear actuator designs have been proposed for accurate position control using different techniques such as displacement feedback, temperature feedback, force feedback and resistance feedback. Each of these techniques has its advantage, as well as constraint and limitation. Self-sensing SMA actuation is considered to be cost-effective as it eliminates the use of external sensor in the system. However, its performance relative to other methods has not been widely discussed. In this study, two techniques were proposed for accurate position control of displacement in the range of 2 mm. The performance of the system using position feedback and self-sensing SMA actuation was evaluated through an experimental test bench developed in this research. The results show that the position feedback system has faster time response and higher accuracy, however, it is costly due to the laser displacement used in the system. The self-sensing SMA actuation produced slower time response and the accuracy was less than 90%. It was found that by providing tension to SMA actuator, the actuation temperature of the SMA actuator increased and the accuracy of the self-sensing system can be improved.

## 1 Introduction

The possibility of using shape memory alloy as actuator is endless. The application encompass various fields from aerospace, robotics, medical, electronics and construction [1]. SMA is deemed attractive due to its high strength to weight ratio and simplicity, resulting in more efficient and reliable system. It can be applied either by using passive or active control. SMA has huge potential for applications that require accurate position control such as piston or valve, robotic hand, antenna pointing and smart aerospace structure. Different techniques have been proposed to produce accurate displacement to suit those applications.

For example in aerospace application, a composite honeycomb structure with embedded SMA wires was designed to detect beam tip displacement for potential applications such as precision space structure and flap shape control [2]. SMA is also suitable to be used as actuator for a reconfigurable parabolic antenna structure due to its ability to produce large deflection [3]. In another study, force controlled was used to produce camber change by measuring the strain on the surface of the structure and controlling with a modified Proportional-Integral-Derivative (PID) controller with anti-windup compensator [4].

Shape memory alloy is also widely used in robotics research. A mechanism for robotic applications was developed using SMA spring using fuzzy controller for position and force [5]. In this system, a closed-loop fuzzy logic controller was able to control the force exerted by the actuator and the position of an attached load. Another example is a highly precise position control of a miniature robot fingertip using SMA and an encoder by employing stiffness and force control measured using strain gauge [6]. SMA was also used for a five-fingered prosthetic hand using tendon-driven under actuated mechanism to produce the required dexterity while keeping the mechanical and control complexity of the device low [7]. Tactile sensors were integrated in the fingertips to improve the overall hand control and a novel resistance feedback control scheme was implemented for the position control.

For automotive applications, a cost-effective mirror actuator was designed and built using shape memory alloy wires integrated with a control algorithm to provide stable and accurate positioning of the external side mirrors

✉ Ermira Junita Abdullah
ermira@upm.edu.my

[1] Department of Aerospace Engineering, Universiti Putra Malaysia, Serdang, Malaysia

[2] CS Centro Stirling, S. Coop, Aretxabaleta, Spain

[8]. SMA has also been considered in a clamping system of a steering column where the shape memory elements control the opening and closing function that presses against the steering jacket [9].

### 1.1 Shape memory alloy actuator for accurate position control

Shape memory alloy wires are able to actuate and produce force when there is change in temperature. This can occur either through conventional heating and Joule heating [10–13]. Shape memory alloy also undergoes phase transformations under loading or temperature change [14, 15]. Upon loading, the shape memory alloy changes into the detwinned martensite phase and it changes into austenite when it is heated. If the shape memory alloy is cooled it will return to the twinned martensite phase.

Many researchers have developed shape memory alloy dynamic model. It describes the change in the SMA's mole fraction, stress and strain with the variation in temperature [16, 17]. The non-linearity and hysteresis behavior of the SMA during heating or cooling which do not coincide making it necessary to introduce compensation and novel techniques to control the response [18–21]. In order to design the SMA actuator, there are challenges that need to be addressed such as the hysteresis behavior and non-linearity of the SMA. A feedback control system design can be employed using various techniques to produce accurate actuation response. Due to the change of several parameters during SMA actuation, it is possible to use position feedback, strain feedback, force feedback or temperature feedback control system to produce accurate actuation.

Position feedback control using SMA actuator can be achieved using a displacement or position sensor. Control technique is used to manipulate the non-linearity of the SMA in order to regulate its stroke. This method provides high accuracy but may be costly due to the sensor used to obtain the position measurement. This method is well established and has been used for various applications. For example the tip position of a composite beam can be actively controlled with robust controller using input measurements from a laser range sensor [12]. Force and position have been proposed to control SMA spring actuation using fuzzy controller [5]. A model-free control (MFC) technique that relies on fast derivative estimation of noisy signals has also been proposed for an SMA-spring based actuator [22]. Precision position control of SMA actuators using modified PID controllers has been demonstrated through experimental investigation [23]. Position control can also be achieved using temperature and strain feedback control but the performance depends on the application. Abdullah et. al adopted a control technique to control the deflection of a composite plate using both temperature and strain feedback [24]. It was found that for their morphing composite plate system, the strain feedback system resulted in better transient response and lower steady state error.

### 1.2 Self-sensing shape memory alloy actuation

Even though it is more effective to directly control the position of system, in the case of SMA there is also a possibility to use its resistivity to control its actuation without the use of external sensors, resulting in a less complex system. There are several factors influencing the electrical resistivity variations but apart from stress and temperature, it is challenging to measure the other factors by real-time control methods resulting in difficulty to apply feedback control techniques [25]. Furthermore, the electrical resistivity variations may be directly or indirectly affected by stress and/or temperature.

Due to the potential and complexity of using resistance feedback for SMA actuation, a number of researches have been focused on resistance characteristic modelling to better understand this behaviour. The resistivity characteristics have been presented earlier in the SMA constitutive equations as developed by Liang and Rogers, as well as Brinson and Huang [16, 26]. Thereafter, a number of studies on the SMA resistivity were presented with resistivity models without taking into account the effect of the phase transformation rate distribution [27–31]. For example, Lynch et. al presented a stress–strain–resistance model with varying applied load and hysteresis effects which was normalized in terms of actuator geometry [32]. Other resistance characteristic model of SMA has also been established using the relative change of resistance [33]. The electrical resistivity of the SMA can be computed using the heating current generated from current amplifier used according to the following equation [34]

$$\rho = R\frac{S}{l} = \frac{U}{I}\frac{V_0}{l^2}$$

where $\rho$ is the electrical resistivity, $R$ is the SMA resistance, $S$ is the cross-sectional area, $l$ is the the length of the SMA wire, $U$ is the voltage, $I$ is the heating current across the SMA wire and $V_0$ is the wire volume which can be considered as constant.

Since the SMA resistance characteristic is more understood with established models available, researchers have developed various control techniques for self-sensing SMA using the change of its resistivity. One example is the self-sensing method established on a 1-DOF manipulator with the discrete time sliding mode controls [35]. A straightforward approach using direct differential resistance feedback has also been proven effective in a one link SMA actuated rotary manipulator employing discrete time

sliding mode control [36]. A control methodology was developed for a shape memory alloy–actuated rotary manipulator using an artificial neural network that is able to accurately model the relationship between the electrical properties and manipulator position [37]. Another method of self-sensing using unscented Kalman Filter based on one-dimensional phenomenological model of SMA wire actuator [38]. Sakagami et. al developed a controller for sensorless SMA actuation to improve the position estimation performance where the resistance model considered the SMA properties of austenite, martensite, and their phase transforms [39]. A new self-sensing-based position control model for the SMA actuator was developed by Lee et. al to improve the accuracy of position control by reducing the effects of hysteresis gap [40].

From the literature, it shows there is great potential in self-sensing technique for accurate SMA actuation. However, it is unclear if its performance is as effective or superior since there has yet to be any comparative study with other displacement feedback control technique especially for applications of very small displacement in the range of $10^{-2}$ m. Thus, the aim of this study is to develop an experimental setup to investigate the feasibility of using self-sensing feedback system for SMA for displacement of 2 mm and to determine how it performs compared to a displacement feedback system. The parameters of interest are the transient response, steady state error and power consumption.

## 2 Methodology

For the requirement of accurate position control within 2 mm, 0.012" Ø SMA wire with length 10 cm was selected. In the experiment a crimped 70 °C Flexinol® 0.012 in Ø, B length of 100 mm ± 1 mm, 13897 Ring Terminal Crimp produced by Dynalloy was selected. This SMA wire length will produce approximately 3% stroke which translates to 2–4 mm displacement. The expected outcome of experiments related to accurate position control using SMA includes calibration of force/position and/or internal resistance/position with respect to temperature and control feedback system to achieve the accurate position control will be developed.

### 2.1 Calibration data for 0.012 in Ø 10 cm SMA wire

The characteristics for the 0.012 in Ø 10 cm SMA wire were first established. It can be used to predict the actuation response of the SMA wire and its behavior. The wire was placed horizontally on a mounting table with one crimped end of the wire secured to the table while the other end was free to move, with a force gauge attached to it. The ambient temperature during the experiment was 27 °C. The SMA was connected in series with a power resistor and power supply, such as the connection shown in Fig. 1. However, the power was supplied directly without using a control feedback. During actuation, the power was increased gradually until it reached 60 °C and then the power was gradually reduced. Various parameters were measured simultaneously including temperature, force, displacement, voltage drop across SMA and voltage drop across power resistor. Since the resistance of the power resistor was 1 Ohm, the current has the same value as voltage drop across the power resistor. The current of the SMA wire was the same as in the power resistor as both are connected in series. Thus, the resistance of the SMA can be calculated using the known values of current and voltage drop across the power resistor.

The change of all parameters against temperature are shown in Figs. 2, 3, 4, and 5. The graphs of Displacement vs Temperature, Force vs Temperature, Resistivity of SMA vs Temperature and Voltage drop across SMA vs Temperature were produced. From the results, it can be seen that the SMA wire was able to produce contraction of 3 mm at temperature of 55 °C with force measurement of 20 N. The resistance was found to be 1.37Ohm at ambient temperature.

In order to produce 2 mm displacement, the SMA wire has to be heated to 47 °C. At this temperature, the SMA wire produced 12 N force, the resistivity was 1.2Ω and voltage drop across SMA was 0.65 V. The rate of change of the displacement with temperature was high as can be seen in Fig. 2. In order to produce an accurate position control, the SMA wire can be pre-loaded with weight at one end in order to lower the rate of change of displacement with temperature. Pre-tension can be designed to provide sufficient force without affecting the subject to be actuated as used in a self-sensing SMA actuator system [41]. Using this technique, it may be utilized for shape memory alloy actuator in meso to micro application.

### 2.2 Experimental procedures

The performance of the accurate position feedback system to achieve 2 mm displacement was tested using a customized test bench developed for this research. For accurate position control of shape memory alloy actuator, a displacement sensor can be used to directly measure the position and as the input to the feedback system. A

**Fig. 1** Calibration setup

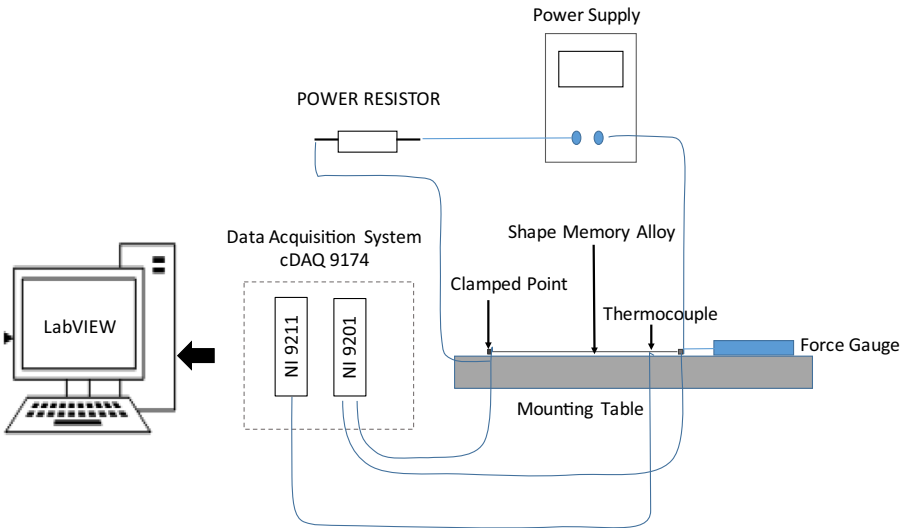


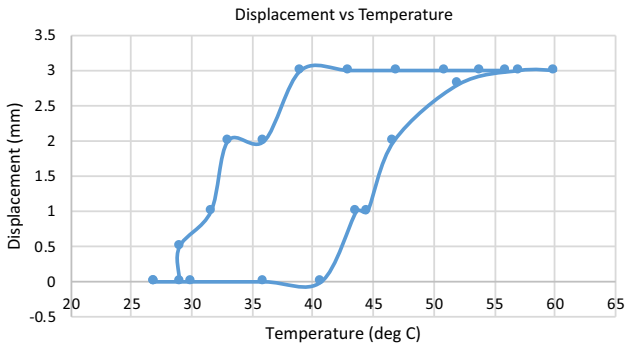


**Fig. 2** Change of displacement with temperature for 10 cm SMA wire

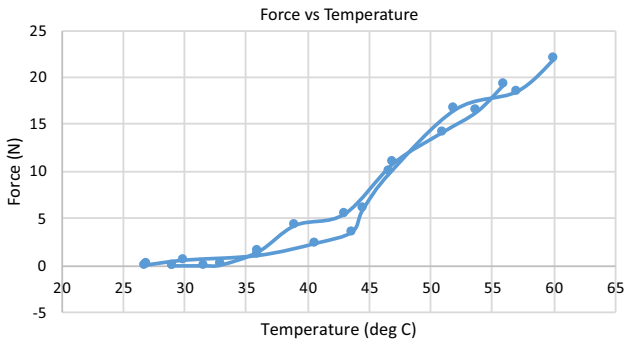


**Fig. 3** Change of force with temperature for 10 cm SMA wire

feedback system using the properties of the SMA can be used to control the displacement of SMA using temperature feedback and control the displacement SMA using force (due to stress/strain) feedback. This system can be improved by using another technique to eliminate the use of sensor. It can be proposed to control the displacement the SMA using self-sensing via voltage drop due to the change in resistivity of the SMA actuator.

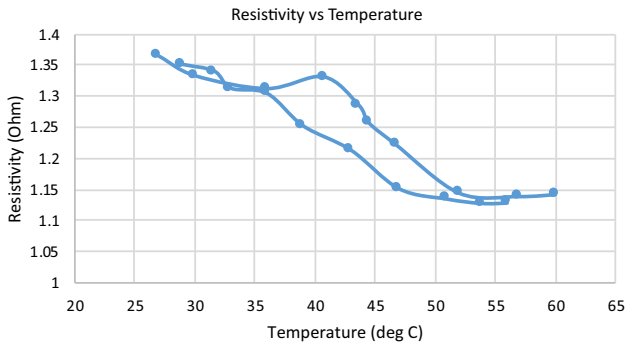


**Fig. 4** Change of resistivity with temperature for 10 cm SMA wire

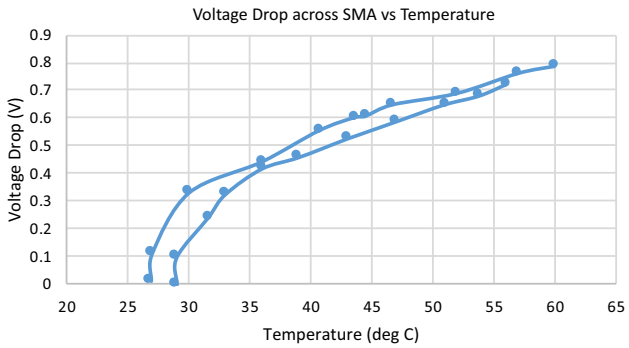


**Fig. 5** Change of voltage drop across SMA with temperature for 10 cm SMA wire

A Proportional-Integral-Derivative controller was selected for accurate position response. The basic PID controller's transfer function is defined as follows

$$G_c(s) = K_p + K_d s + \frac{K_i}{s}$$

where $K_p$, $K_i$ and $K_d$ are real constants. In the accurate position control system developed here, the gains were tuned to meet the system requirements

For the displacement feedback system as shown in Fig. 6, where $l_{ref}$(t) is the desired displacement, and $l$(t) is the actual or measured displacement of the SMA actuation. The difference between $l_{ref}$(t) and $l$(t) is the control error, $e$. For the displacement feedback system, the control errors are defined as

$$e = l_{ref} - l$$

Similarly, the block diagram for the PID controller of the self-sensing system is shown in Fig. 7 where $u_{ref}$ (t) is the desired voltage, and $u$(t) is the actual or measured voltage drop across the SMA wire. This voltage value corresponds to the displacement of the SMA wire as established in the calibration test. The control error, $e$, is the difference between $u_{ref}$(t) and $u$(t). For the self-sensing system, the control errors are defined as

$$e = u_{ref} - u$$

In the test bench the crimped ends of the SMA were clamped at both ends with one fixed and the other was free to move. A thermocouple secured with Kapton tape was used to measure the temperature of SMA during actuation, as shown in Fig. 8. A laser position laser positioning measurement system (Panasonic HG-C1050-P, 30 microns resolution) was used to measure the displacement during SMA actuation for the displacement feedback system and was placed at one end of the clamp. For the self-sensing system, a 1Ohm/100 W power resistor was connected in series with the SMA wire. The voltage drop across the resistor can be measured and the corresponding current of the system can be estimated as it is the same across all components in a series circuit.

National Instruments hardware was used for the data acquisition as shown in Fig. 9. The CompactRIO 9045 chassis was used in this experiment in order to achieve faster response employing its field-programmable gate array (FPGA). NI 9201, NI 9474 and NI 9213 modules were required in this experimental setup to measure analog inputs as SMA voltage drop, system voltage and displacement signal; to control digital outputs as laser calibration signal and relay command and to measure SMA temperature during all the process respectively. The wiring diagram of the electrical connections for the displacement feedback system and self-sensing system is shown in Fig. 10. For both feedback systems, a solid state relay type SSR-25DD (3-10VDC 20A 60VDC) was used in the circuit for power control.

## 2.3 Calibration of feedback system

A set of experiments to calibrate both the displacement feedback control system and self-sensing control system was conducted using the test bench that has been developed. The SMA wire was pre-loaded with different weights at the free end of the SMA wire to produce tension. Three different weights were used 500 g, 700 g and 800 g. The results of the calibration for the displacement feedback system are presented in Fig. 11. It was found that pre-loading the wire didn't affect the change of voltage drop across the SMA wire with temperature during activation. The calibration data of these parameters is similar to the unloaded SMA wire as in Fig. 5. During calibration of the unloaded SMA wire, it was found that 2 mm displacement occurred at 47 °C. At this temperature, the voltage drop was 0.65 V. For the pre-loaded SMA wire, voltage drop across SMA increased significantly with increase of the pre-load ranging from 0.65 to 0.75 V for 2 mm displacement. The temperature for the pre-loaded SMA wire was not the same as the unloaded wire. For the SMA wire pre-loaded with 500 g, the displacement reached 2 mm at higher temperature of 52 °C. For the SMA wire pre-loaded with 700 g, it reached 2 mm displacement at 54 °C and for the SMA wire pre-loaded with 800 g, it reached 2 mm displacement at 57 °C. In general, the rate of change of displacement also reduced with increase in the pre-load weight attached to the SMA wire.

For the self-sensing feedback system, the results of the calibration are presented in Fig. 12. It was found that pre-loading the wire didn't affect the change of voltage drop with temperature during activation. The calibration data of these parameters is similar to the unloaded SMA wire as in Fig. 5. During calibration of the unloaded SMA wire, it was found that 2 mm displacement occurred at 47 °C. At this temperature, the voltage drop was 0.65 V. For the pre-loaded SMA wire, this was also true for all weights used where the voltage drop across SMA was approximately

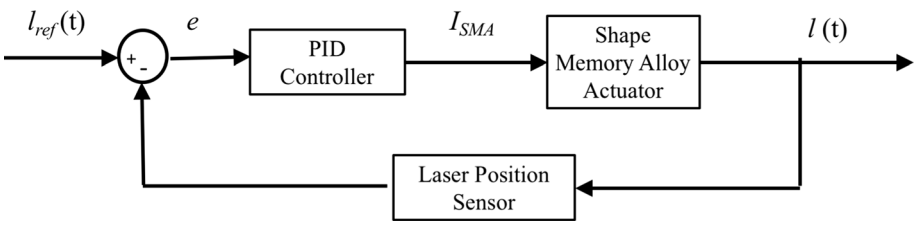


**Fig. 6** Block diagram for accurate position control using displacement feedback system

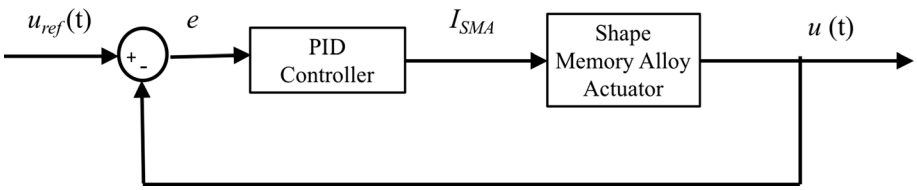


**Fig. 7** Block diagram for accurate position control using self-sensing system

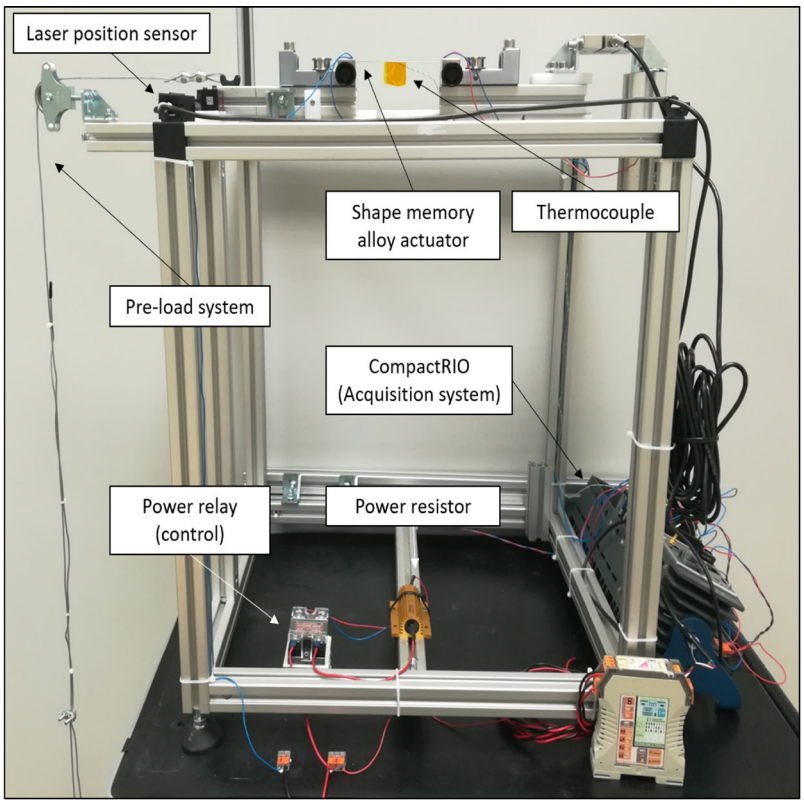


(a)

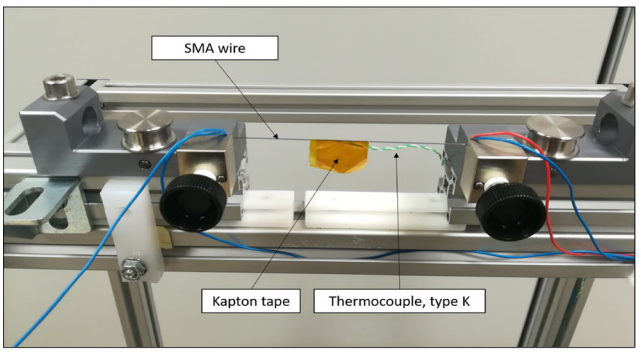


(b)

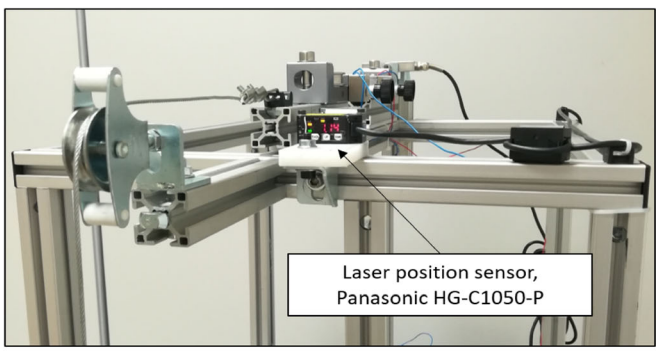


(c)

**Fig. 8** **a** Experimental setup of the accurate position control of shape memory alloy actuator, **b** SMA wire assembly with thermocouple attachment and **c** Side view: Laser position sensor located at one end of the test bench

0.64–0.69 V for 2 mm displacement. However, the temperature for the pre-loaded SMA wire was not the same as the unloaded wire. For the SMA wire pre-loaded with 500 g, the displacement reached 2 mm at higher temperature of 52 °C. For the SMA wire pre-loaded with 700 g, it reached 2 mm displacement at 53 °C and for the SMA wire pre-loaded with 8 N, it reached 2 mm displacement at 55 °C.

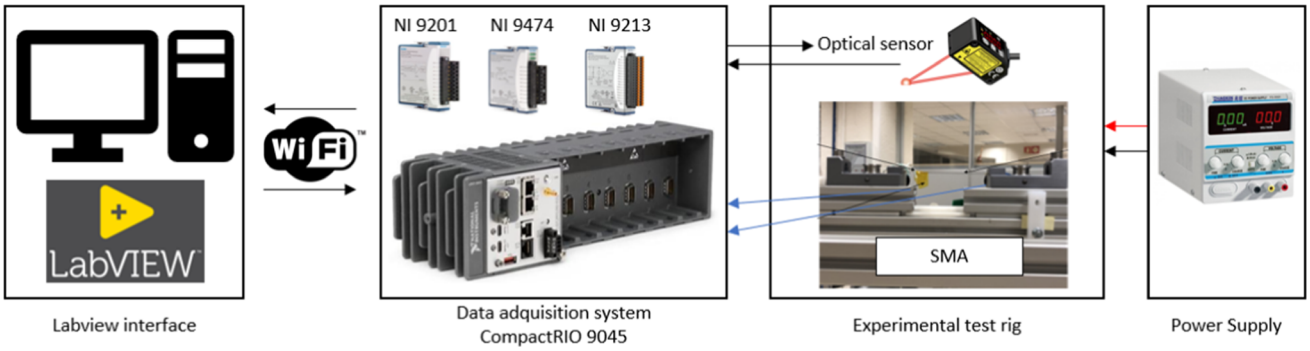


**Fig. 9** Data acquisition and control systems hardware

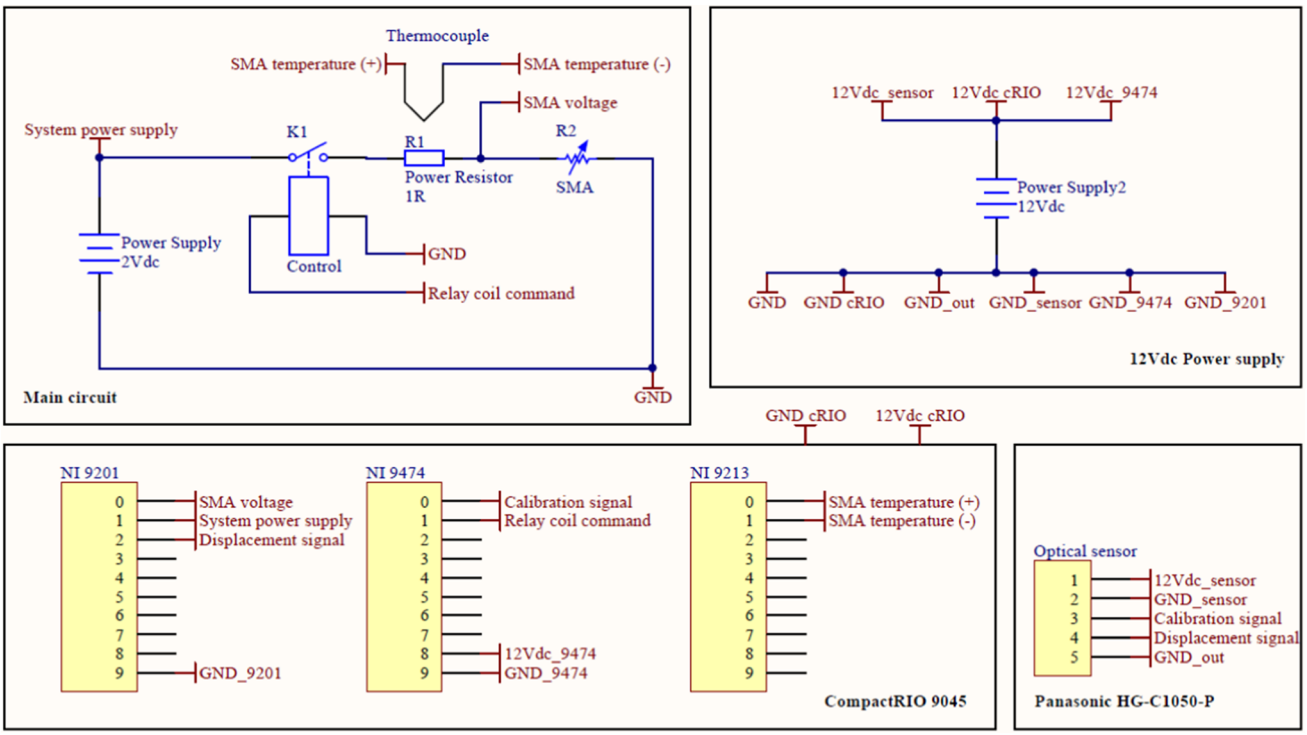


**Fig. 10** Wiring diagram of electrical connection for the SMA accurate position control system for displacement/self-sensing control

It can be seen from the calibration data that the displacement feedback system has lower hysteresis for the change of displacement with voltage. In the case of the self-sensing system, the hysteresis was large where the voltage during heating and cooling cycle at 2 mm displacement were 0.6 V and 0.4 V respectively. This indicates that accuracy of the position may be better for the displacement feedback system as the value of displacement during heating was close to the displacement value during the cooling cycle. For the displacement feedback system, the slope for the displacement against temperature for displacement between 2 and 3 mm reduced only slightly with increase of the pre-load, indicating slower rate of change of displacement of the SMA wire. However, for the self-sensing system the rate of change of displacement reduced significantly with the increase in the pre-load weight attached to the SMA wire. The slope for the displacement against temperature for displacement between 2 and 3 mm was lowest for the SMA wire pre-loaded with 800 g weight. By adding tension to the SMA actuator may improve the accuracy of the self-sensing system.

## 3 Results and discussions

Both systems with pre-loading were tested to compare their step response in achieving accurate position of 2 mm. The results for both systems are shown in Figs. 13, 14, and 15. For the step response test for the system with 500 g pre-loading, it was found that the displacement feedback

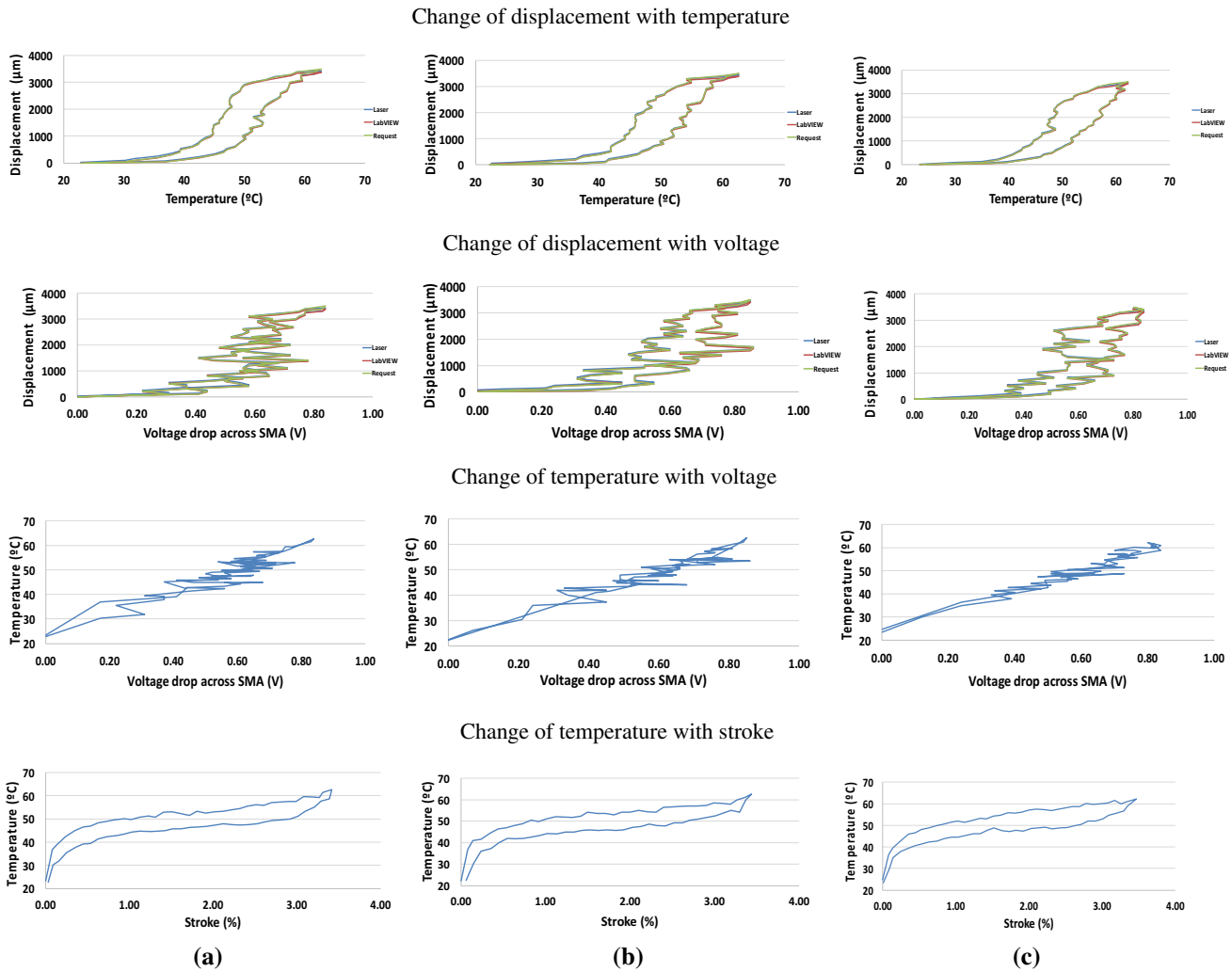


**Fig. 11** Calibration of 10 cm SMA wire using displacement feedback control with pre-loading **a** 500 g, **b** 700 g and **c** 800 g

system's steady state error was 1% while the self-sensing system had slow response and steady state error of 15%. The average temperature of the displacement feedback system was lower at 52 °C compared to the self-sensing system which had an average temperature of 55 °C. For the displacement feedback system, the initial power was high with voltage of 1 V and current of 0.8A however the steady state power consumption was lower with voltage of 0.65 V and current of 0.55 A. The average power consumption for the self-sensing system was almost the same with voltage of 0.64 V and current of 0.55 A.

For the case with 700 g pre-loading, it was found that the displacement feedback system's steady state error was also 1%. By increasing the pre-loading, the accuracy of the self-sensing system improved as the steady state error reduced to 11%. The average temperature of the displacement feedback system was lower at 53 °C compared to the self-sensing system which had an average temperature of 55 °C. For the displacement feedback system, the initial power was high with voltage of 1 V and current of 0.8A, however the steady state power consumption was lower with voltage of 0.67 V and current of 0.57 A. The average power consumption for the self-sensing system was almost the same with voltage of 0.66 V and current of 0.57 A. Similar findings were found when the pre-loading was increased to 800 g. The pre-loading didn't affect the displacement feedback system accuracy as the steady state error remained at 1%. However, the increase in pre-loading value caused the self-sensing system to be less accurate, with higher steady state error of 17.5%. The average temperature of the displacement feedback system was lower at 54 °C compared to the self-sensing system which had an average temperature of 57 °C. For the displacement feedback system, the initial power was high with voltage of 1 V and current of 0.8A however the steady state power consumption was lower

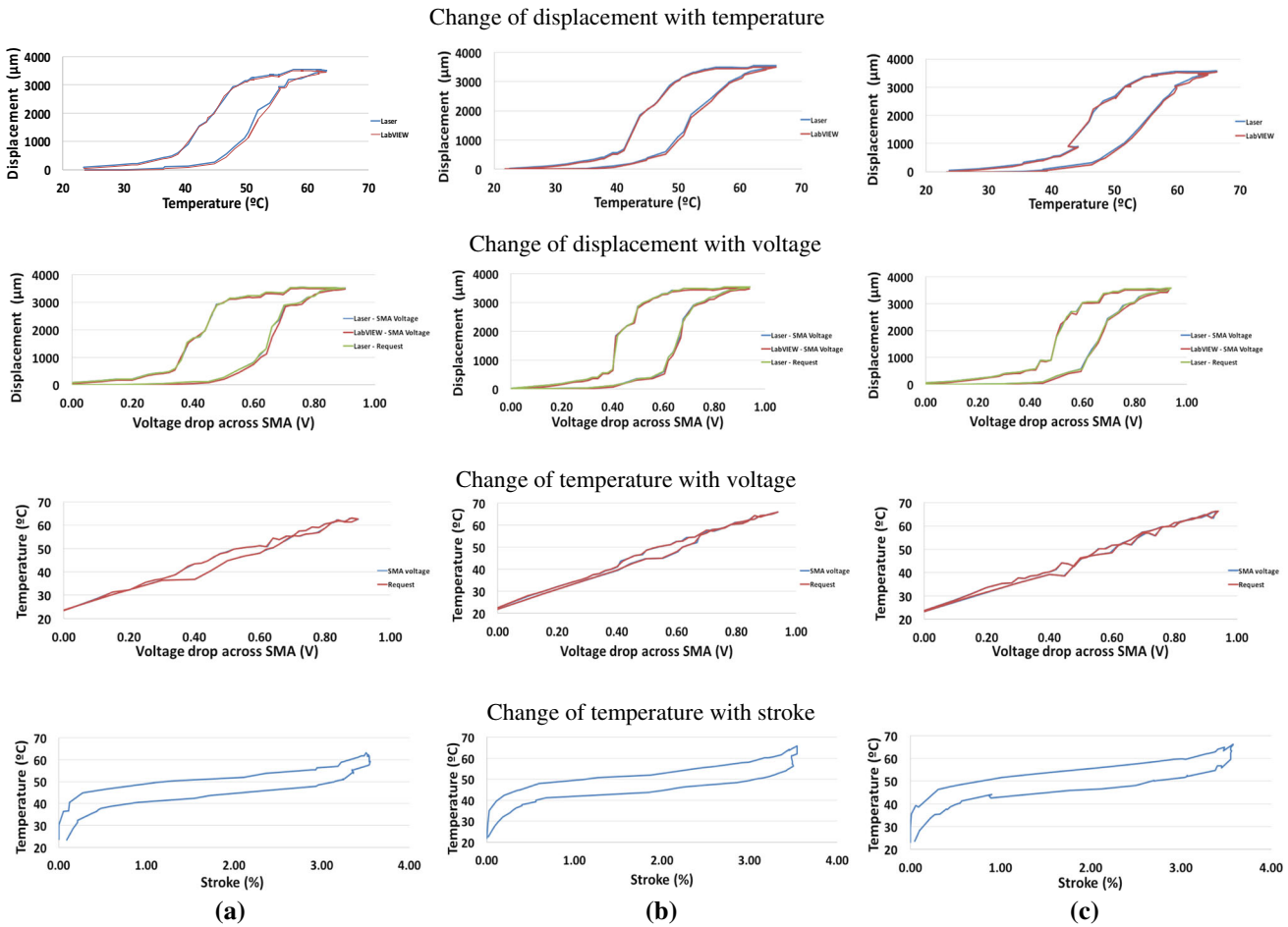


**Fig. 12** Calibration of 10 cm SMA wire using self-sensing feedback control with pre-loading **a** 500 g, **b** 700 g and **c** 800 g

with voltage of 0.68 V and current of 0.58A. In this case, the average power consumption for the self-sensing system was slightly higher with voltage of 0.69 V and current of 0.6 A.

The displacement feedback system has excellent performance in terms of time response and accuracy with steady state error of 1% for all conditions. The self-sensing system was less accurate with the step response steady state error of 15%. In all the tests, it was found that the displacement feedback system consumed high initial power to drive the system resulting in high rise time compared to the self-sensing system. The average temperature for displacement feedback was lower compared to the temperature of the self-sensing system which contributed to the difference in stroke of SMA for both systems where the displacement feedback system produced lower stroke. The higher stroke produced in the self-sensing system caused the displacement to be higher than 2 mm resulting in the response to be less accurate with larger steady state error. The change in pre-loading had small effect on the displacement feedback system, however it improved the accuracy of the self-sensing feedback where the steady state error reduced to 11% for the system with 700 g pre-loading. However, by increasing the pre-loading further and also the input voltage caused the SMA's temperature to rise and the stroke to increase. This resulted in higher steady state error of the self-sensing system when the pre-loading was increased to 800 g.

## 4 Conclusions

An experimental test bench was developed for accurate position of very low displacement in the range of 2 mm using shape memory alloy actuator. Various feedback systems can be developed for position control using shape memory alloy actuator such as the displacement, resistivity, force or temperature of the SMA actuator. In the research work presented here, a displacement feedback control system and a self-sensing feedback control system were designed and their performance were compared. It was expected that the displacement feedback system will

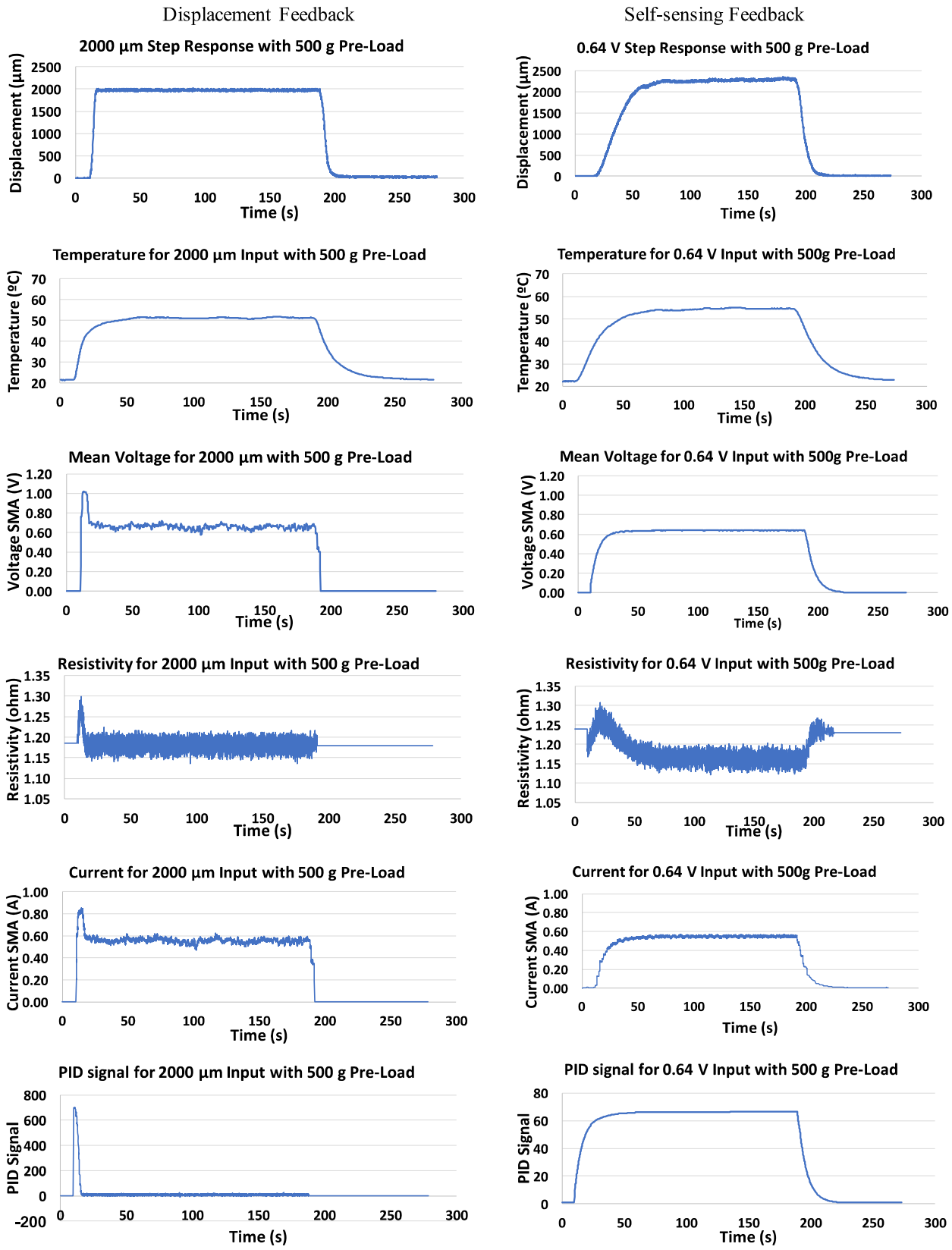


**Fig. 13** Step response for displacement feedback and self-sensing feedback system with pre-loading of 500 g

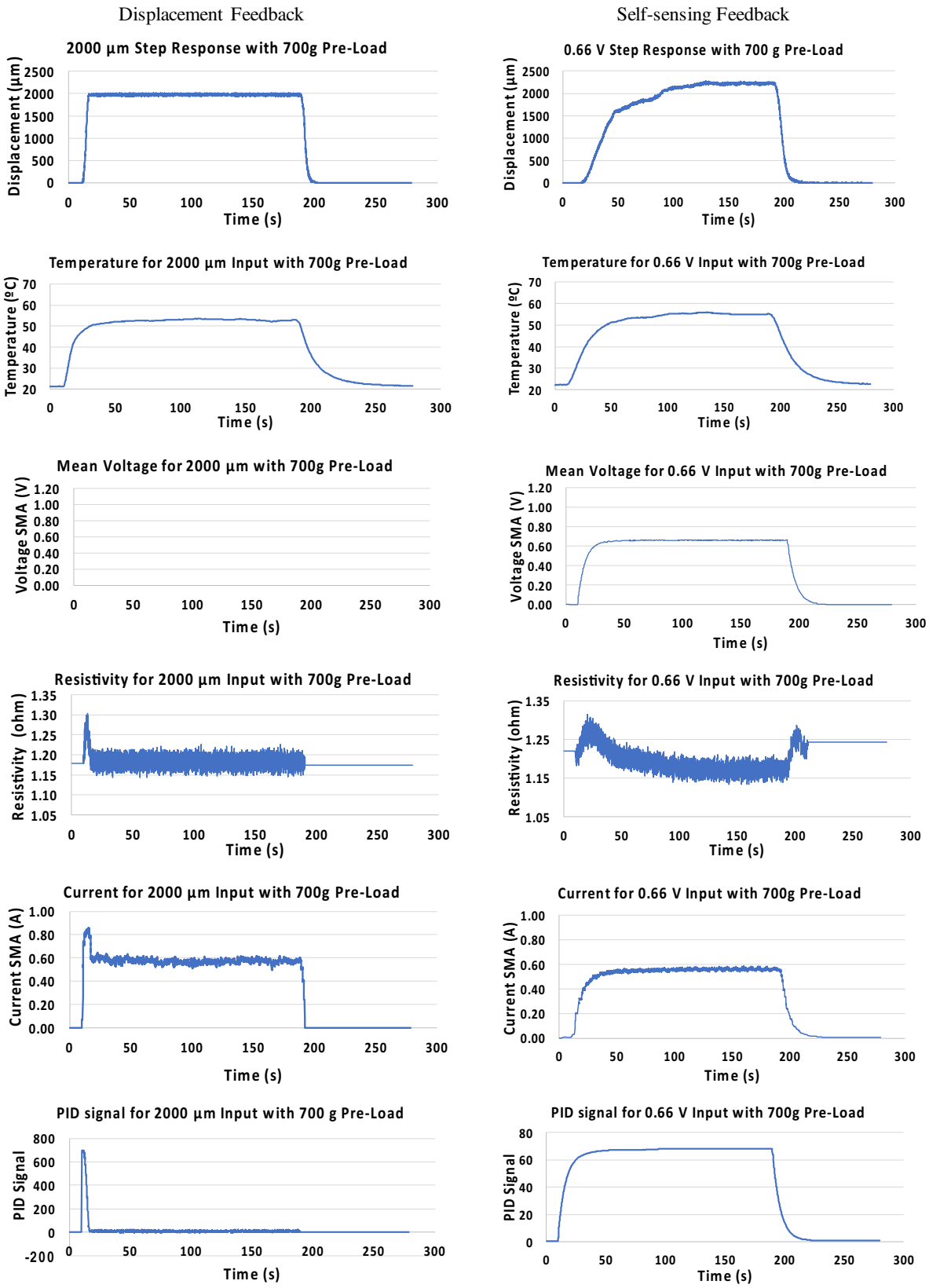


**Fig. 14** Step response for displacement feedback and self-sensing feedback system with pre-loading of 700 g

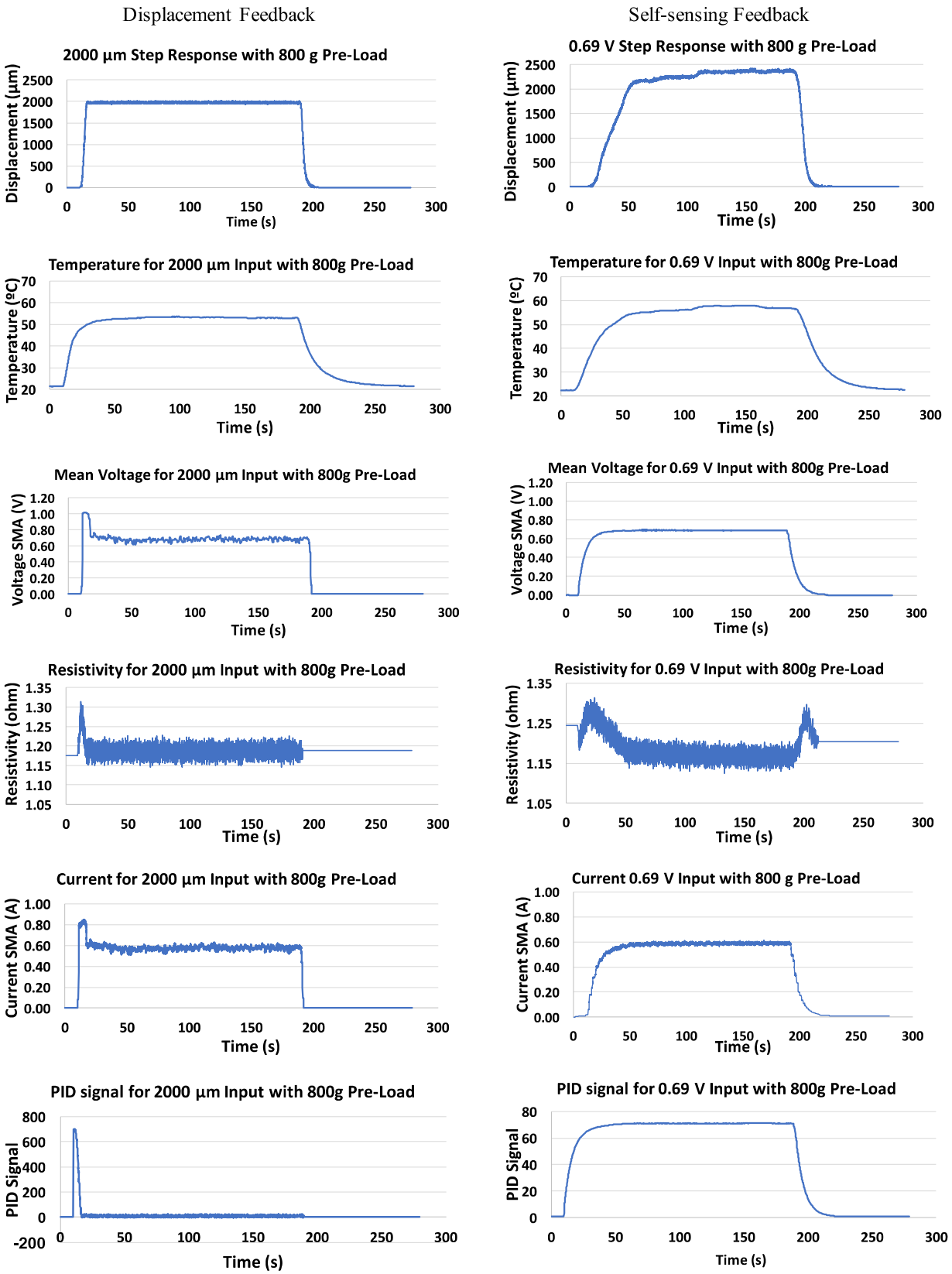


**Fig. 15** Step response for displacement feedback and self-sensing feedback system with pre-loading of 800 g

produce better accuracy but the self-sensing feedback control may potentially reduce the system's cost as it eliminates the use of sensor. Thus, this study seeks to investigate the self-sensing system's accuracy as compared to the displacement feedback system.

Laser displacement sensor was used to obtain position measurements and provided input to the displacement feedback system. For the self-sensing system, the voltage drop across the SMA was used as input measurement to the system. The displacement feedback system has excellent transient response performance and accuracy with steady state error of 1% for all conditions. The self-sensing feedback was less accurate with slow response time. However, the accuracy of the self-sensing system was improved with pre-loading the SMA actuator. The steady state error reduced from 15 to 11% when the pre-loading was increased from 500 to 700 g.

Using the experimental test bench presented here, the displacement feedback system performed better than the self-sensing system for 2 mm position control using shape memory alloy. However, the self-sensing system feedback system can be improved by providing tension to the wire as demonstrated in the experimental investigation. The results demonstrate the feasibility of replacing the displacement feedback system with the more cost-effective self-sensing actuation system. In the experimental setup for accurate position control proposed here, the use of laser displacement sensor can be eliminated. This technique requires less component, thus reducing the initial cost of the system as well as the overall system's cost in the long run. The self-sensing system can be considered to be more cost-effective compared to other actuation system that requires external position measuring device such as Linear Variable Differential Transformer (LVDT), infrared sensor, laser sensor and strain gauge with its associated costs of purchasing, maintenance, power consumption and the electronics and software development of the measurement system.

**Acknowledgements** The authors would like to acknowledge that the research findings presented in this paper was funded by CS Centro Stirling, S. Coop and Research University Grant Scheme (RUGS) UPM/700-2/1/GPB/2017/9530800 from Universiti Putra Malaysia.

## References

1. Savi M, Paiva A, de Araujo A, de Paula CJ (2016) Shape memory alloys. In: Lopes Junior V, Savi SV Jr. (eds) Dynamics of smart systems and structures. Springer, Cham, pp 155–188
2. Song G, Kelly B, Agrawal BN (2000) Active position control of a shape memory alloy wire actuated composite beam. Smart Mater Struct 9:711–716
3. Kalra S, Bhattacharya B, Munjal BS (2017) Design of shape memory alloy actuated intelligent parabolic antenna for space applications. Smart Mater Struct 26:095015
4. Bil C, Massey K, Abdullah EJ (2013) Wing morphing control with shape memory alloy actuators. J Intell Mater Syst Struct 24(7):879–898
5. de Oliveira S, Silva SA, Souto CR, Ries A (2018) Experimental characterization and control of a force actuator based on shape memory alloy wire. J Control Autom Electr Syst 29:670–676
6. Hino T, Maeno T (2004) Development of a miniature robot finger with a variable stiffness mechanism using shape memory alloy. Internationalsimposium on robotics and automation 2004. Querétaro, México
7. Andrianesis K, Tzes A (2015) Development and control of a multifunctional prosthetic hand with shape memory alloy actuators. J Intell Robot Syst 78,:257–289
8. Williams E, Shaw A, Elahinia G (2010) Control of an automotive shape memory alloy mirror actuator. Mechatronics 20(5):527–534
9. Gheorghita V, Gümpel P, Strittmatter J, Anghel C, Heitz T, Senn M (2013) Usingshape memory alloys in automotive safety systems. In: SAE-China, FISITA (ed) Proceedings of theFISITA 2012 world automotive congress. Lecture notes in electrical engineering, Vol 195. Springer, Berlin, Heidelberg
10. Dong Y, Boming Z, Jun L (2008) A changeable aerofoil actuated by shape memory alloy springs. Mater Sci Eng A 485(1):243–250
11. Lara-Quintanilla A, Hulskamp AW, Bersee H (2013) A high-rate shape memory alloy actuator for aerodynamic load control on wind turbines. J Intell Mater Syst Struct 24(15):1834–1845
12. Song G, Lam PC, Srivatsan TS, Kelly B, Agrawa BN (2000) Application of shape memory alloy wire actuator for precision position control of a composite beam. J Mater Eng Perform 9(3):330–333
13. Chaitanya SK, Kaliaperumal D (2014) Design and investigation of a shape memory alloy actuated gripper. Smart Struct Syst 14(4):541–558
14. Kaufman L, Cohen M (1958) Thermodynamics and kinetics of martensitic transformations. In: Chalmers B, King R (eds) Progress in metal physics. Pergamon Press, London
15. Nishiyama Z (1978) Martensitic transformation, 1st edn. Elsevier, Amsterdam
16. Liang C, Rogers CA (1990) One-dimensional thermomechanical constitutive relations for shape memory materials. J Intell Mater Syst Struct 1:207–234
17. Jayender J, Patel RV, Nikumb S (2008) Modeling and control of shape memory alloy actuators. IEEE Trans Control Syst Technol 16(2):279–287
18. Schiedeck F, Mojrzisch S (2011) Frequency-domain control design for shape memory alloy actuators. Sens Actuators A Phys 169(1):133–140
19. Feng Y, Rabbath CA, Hong H, AlJanaideh M, Su CY (2010) Robust control for shape memory alloy micro-actuators based flap positioning system. Proceedings of the 2010 American Control Conference. IEEE, Baltimore
20. Pai A, Riepold M, Trachtler A (2016) A model extended temperature and strain controller modulated with PWMfor precision position control of shape memory alloy actuators. IEEE International Conference on Advanced Intelligent Mechatronics (AIM). IEEE, Banff
21. Zakerzadeh MR, Sayyaadi H (2013) Precise position control of shape memory alloy actuator using inverse hysteresis model and model reference adaptive control system. Mechatronics 23(8):1150–1162
22. Gédouin PA, Delaleau E, Jean-Matthieu Bourgeot JM, Join C, Chirani SA, Calloch S (2011) Experimental comparison of classical PID and model-free control: position control of a shape memory alloy active spring. Control Eng Pract 19(5):433–441

23. Park S, Hwang D (2020) An experimental study on precision positioning characteristics of shape memory alloy actuator. Microsyst Technol. https://doi.org/10.1007/s00542-020-04853-2
24. Abdullah EJ, Gaikwad PS, Azid N, Majid A, Rafie DL M (2018) Temperature and strain feedback control for shape memory alloy actuated composite plate. Sens Actuators A Phys 283:134–140
25. Zhang JJ, Yin YH, Zhu JY (2013) Electrical resistivity-based study of self-sensing properties for shape memory alloy-actuated artificial muscle. Sensors 13(10):12958–12974
26. Brinson LC, Huang MS (1996) Simplifications and comparisons of shape memory alloy constitutive models. J Intell Mater Syst Struct 7:108–114
27. Yan S, Zhang Y, Wang W, Yu Z (2008) Electrical resistance-strain model for shape memory alloys. J Shenyang Jianzhu Univ Nat Sci 24:980–984
28. Cui D, Li H, Song G (2008) Study on electrical resistance properties of shape memory alloy. J Build Mater Struct 11:567–573
29. Cui D, Song G, Li H (2010) Modeling of the electrical resistance of shape memory alloy wires. Smart Mater Struct 19:055019
30. Xu L, Wang R, Zhang S (2010) Electrical resistance properties of Ni–Ti shape memory alloy fiber in phase transformation. Text Res J 31:15–19
31. Zhang J, Chen B, Geng L, Chen S, Wu H (2011) Design of control system for SMA actuator based on resistance feedback. Microprocessors 35:91–93
32. Lynch B, Jiang XX, Ellery A, Nitzsche F (2016) Characterization, modeling and control of Ni–Ti shape memory alloy based on electrical resistance feedback. J Intell Mater Syst Struct 27:2489–2507
33. Lu Y, Zhang R, Xu Y, Wang L, Yue H (2020) Resistance characteristics of SMA actuator based on the variable speed phase transformation constitutive model. Materials 13:1479
34. Faulkner M, Amalraj J, Bhattacharyya A (2000) Experimental determination of thermal and electrical properties of Ni–Ti shape memory wires. Smart Mater Struct 9:632–639
35. Ruth D, Kaliaperumal J (2017) Shape memory alloy wire for self-sensing servo actuation. Mech Syst Signal Process 83(15):36–52
36. Josephine Selvarani Ruth D, Dhanalakshmi K, Nakshatharan S (2015) Bidirectional angular control of an integrated sensor/actuator shape memory alloy based system. Measurement 69:210–221
37. Narayanan P, Elahinia M (2016) Control of a shape memory alloy–actuated rotary manipulator using an artificial neural network–based self-sensing technique. J Intell Mater Syst Struct 27(14):1885–1894
38. Gurung H, Banerjee A (2016) Self-sensing shape memory alloy wire actuator based on unscented Kalman filter. Sens Actuators A Phys 251:258–265
39. Sakagami T, Seki K, Iwasaki M (2019) Sensorless position control based on resistance and heat transfer models in shape memory alloy actuators. IEEE/ASME Int Conf Adv Intell Mechatron 2019:217–222
40. Lee SH, Kim SW (2019) Improved position control of shape memory alloy actuator using the self-sensing model. Sens Actuators A 297:111529
41. Lan CC, Fan CH (2010) Investigation on pretensioned shape memory alloy y. Actuators for force and displacement self-sensing. IEEE International Workshop on Intelligent Robots and Systems (IROS). IEEE, Taipei